coatings

MDPI

Article

Competitive Mechanism of Alloying Elements on the Physical Properties of $Al_{10}Ti_{15}Ni_{x1}Cr_{x2}Co_{x3}$ Alloys through Single-Element and Multi-Element Analysis Methods

Yu Liu [1,2], Lijun Wang [1], Juangang Zhao [1], Zhipeng Wang [3], Ruizhi Zhang [1,*], Yuanzhi Wu [1,*], Touwen Fan [1] and Pingying Tang [4]

[1] Research Institute of Automobile Parts Technology, Hunan Institute of Technology, Hengyang 421002, China; liuyu@hnit.edu.cn (Y.L.)
[2] College of Materials Science and Engineering, Hunan University, Changsha 410082, China
[3] State Key Laboratory of Advanced Design and Manufacturing for Vehicle Body, Hunan University, Changsha 410082, China
[4] Key Laboratory of New Electric Functional Materials of Guangxi Colleges and Universities, Nanning Normal University, Nanning 530023, China
* Correspondence: 2006000495@hnit.edu.cn (R.Z.); ranco007@163.com (Y.W.)

Abstract: Altering the content of an alloying element in alloy materials will inevitably affect the content of other elements, while the effect is frequently disregarded, leading to subsequent negligence of the common influence on the physical properties of alloys. Therefore, the correlation between alloying elements and physical properties has not been adequately addressed in the existing studies. In response to this problem, the present study focuses on the $Al_{10}Ti_{15}Ni_{x1}Cr_{x2}Co_{x3}$ alloys and investigates the competitive interplay among Ni, Cr, and Co elements in the formation of physical properties through a single-element (SE) analysis and a multi-element (ME) analysis based on the first principles calculations and the partial least squares (PLS) regression. The values of C_{11} and C_{44} generally increase with the incorporation of Ni or Cr content in light of SE analysis, which is contrary to the inclination of ME analysis in predicting the impact of Ni and Cr elements, and the Ni element demonstrates a pronounced negative competitive ability. The overall competitive relationship among the three alloying elements suggests that increasing the content of Ni and Cr does not contribute to enhancing the elastic constants of alloys, and the phenomenon is also observed in the analysis of elastic moduli. The reason is that the SE analysis fails to account for the aforementioned common influence of multiple alloying elements on the physical properties of alloys. Therefore, the integration of SE analysis and ME analysis is more advantageous in elucidating the hidden competitive mechanism among multiple alloying elements, and offering a more robust theoretical framework for the design of alloy materials.

Keywords: alloying elements; common influence; single-element analysis; multi-element analysis; competitive mechanism

Citation: Liu, Y.; Wang, L.; Zhao, J.; Wang, Z.; Zhang, R.; Wu, Y.; Fan, T.; Tang, P. Competitive Mechanism of Alloying Elements on the Physical Properties of $Al_{10}Ti_{15}Ni_{x1}Cr_{x2}Co_{x3}$ Alloys through Single-Element and Multi-Element Analysis Methods. *Coatings* **2024**, *14*, 639. https://doi.org/10.3390/coatings14050639

Academic Editor: Carlos Jose Macedo Tavares

Received: 2 April 2024
Revised: 15 May 2024
Accepted: 16 May 2024
Published: 18 May 2024

1. Introduction

Alloy materials, encompassing a diverse array of alloy components, often exhibit exceptional physical properties, e.g., high strength [1], good ductility [2], outstanding thermal stability [3], superior corrosion and wear resistance [4,5], excellent electrical and thermal conductivity [6,7]. The modulation of alloying element content can effectively control these aforementioned characteristics, as alterations in alloy composition trigger a cascade of intrinsic property transformations within the alloy materials. For instance, Al, Ta and Nb elements induce phase transformation [8–10], Si and B elements refine grain structure [11,12], C, Mo and Ti elements promote nanotwin generation [13–15], Cu, Cr, and S elements alleviate or accelerate component segregation [16–18], and Zn and W elements

enhance solid solution strengthening [19,20]. It can be seen that the internal structural characteristics of alloy materials can be directly or indirectly influenced by adjusting the content of alloying elements, thereby impacting the physical properties of alloy materials. Therefore, relevant exploration is warranted to investigate the potential regular effects of varying alloying element content on the physical properties of alloy materials.

To this end, researchers have consistently pursued the exploration of alloy materials with excellent physical properties by effectively controlling the content of alloying elements, and then uncovering the influence trend. Zhang et al. [21] incorporated the Ag element into the Al-33Zn-2Cu alloy and observed a linear increase in both yield strength and tensile strength with increasing Ag content. Ye et al. [22] observed that the hardness of $CuCoFeNiTi_x$ high-entropy alloy (HEA) gradually increased with the increase in Ti content, while the ductility gradually decreased. Nguyue et al. [23] found that the phase structure of $Al_xFeMnNiCrCu_{0.5}$ HEA exhibits multiple transformations with increasing Al content, leading to parabolic fluctuations in the tensile properties of the alloy. Luo et al. [24] calculated that the Young's modulus, bulk modulus and hardness of Fe-Mn-Al alloy showed an overall decreasing trend with the increase in Mn content. Liu et al. [25] simulated that increasing Mn content in $CrFeCoNiMn_x$ ($0 \leq x \leq 3$) HEAs will improve the required fracture energy for their crystal cell structure. Meanwhile, researchers controlled the content of diverse alloying elements and conducted corresponding investigations. The content of Mn, C, and Al elements in Fe-Mn-Al-C low-density steels was simultaneously increased by Wang et al. [26]. The results demonstrated that the value of yield strength declines with the increase in Mn content, and rises with higher Al and C contents. The study conducted by Li et al. [27] demonstrates that the influences of Cu and W on CoNiCuMoW HEAs are opposite, with an observed enhancement in thermodynamic stability and dislocation energy factor resulting from increased W content. And Fan et al. [28] independently studied the effects of Al and Cu contents on the mechanical properties of $(FeCrNiCo)Al_xCu_y$ HEAs, observing a significant increase in hardness and yield strength with higher Al content, while noting a substantial reduction in fracture strength with increased Cu element presence. Obviously, the variation in alloy element content in alloy materials has a regular impact on physical properties. Through the regularity analysis, it is possible to identify optimal ratios of alloy elements that yield superior physical properties.

However, based on the aforementioned researches, it can be observed that whether through manipulation of a single alloying element or multiple alloying elements, the final analysis solely focuses on the impact of altering the content of a single alloy element on the physical properties of alloy materials. The potential effect of altering the content of a single alloy element on other alloy elements and their collective influence on the physical properties of alloy materials are disregarded. Therefore, the regulatory strategies of the aforementioned alloying elements have not been adequately investigated. Addressing this issue, the present study employs a combination of first principles calculations and partial least squares (PLS) regression to simultaneously regulate the content of Ni, Cr, and Co elements in $Al_{10}Ti_{15}Ni_{x1}Cr_{x2}Co_{x3}$ alloys, and the physical properties, lattice constant, elastic constants, elastic moduli, Vichers hardness, and yield strength, are calculated and discussed. Subsequently, the differences between single-element (SE) analysis and multi-element (ME) analysis were explored for the same alloying element, revealing the competition mechanism between alloying elements and providing more reliable theoretical guidance for further experimental preparation.

2. Materials and Computational Methods

The exact muffin-tin orbitals (EMTO) and coherent potential approximation (CPA) methods based on the density functional theory were employed to implement the first principles calculations of $Al_{10}Ti_{15}Ni_{x1}Cr_{x2}Co_{x3}$ alloys [29–31]. In which, the full charge density technique is chosen to calculate the total energy [32]. The Kohn-Sham equations [33,34] is used to solve the single-electron equations of optimized overlapping muffin-tin potential spheres. To represent the exchange-correlation function, the Perdew–Burke-Ernzerhof

(PBE) generalized gradient approximation (GGA) is utilized [35]. The paramagnetic state is characterized using the disordered local moment model [36], while ensuring convergence accuracy in the Brillouin zone by setting 25 × 25 × 25 inequivalent k-points for integration calculations. Meanwhile, the EMTO basis group optimizes the convergence of s, p, d, and f orbitals [37], and the electrostatic correction of the single-site CPA method is implemented using the screened impurity model, employing a screening parameter of 0.7 [38]. As a measure to ensure the accuracy of calculated results, we solve for the Green's function at 16 complex energy points located on the Fermi surface [39]. By fitting the predicted energy-volume data using a Morse-type function and then deriving the state equation [40]. Consequently, the results enable us to determine the equilibrium volume and lattice constant of $Al_{10}Ti_{15}Ni_{x1}Cr_{x2}Co_{x3}$ alloys.

Subsequently, the PLS regression [41] is utilized to investigate the disparity in the impact of one alloying element between SE and ME analyses according to the calculated results of first principles calculations. The PLS regression is a sophisticated statistical method that integrates various analytical techniques such as multiple linear regression analysis [42], principal component analysis [43], canonical correlation analysis [44], and others. It adeptly tackles challenges related to multicollinearity, high-dimensional variables, and limited sample sizes [45]. For this study, the contents of Al and Ti elements in $Al_{10}Ti_{15}Ni_{x1}Cr_{x2}Co_{x3}$ alloys are, respectively, fixed at 10 at% and 15 at%, and the Ni, Cr, and Co contents are control variables in the range of 0–75 at%. Clearly, the modification of one element within the Ni, Cr, and Co inevitably results in an alteration in the content of other elements. Therefore, a main control (MC) element is established with a 15 at% content increment for each calculation step, while the other two elements serve as slave control (SC) variables with equivalent content values. For instance, the red dotted line with a circular box is shown in Figure 1, Cr is the MC element, with its content C_{Cr} gradually increasing from 0 at% to 75 at% in increments of 15 at%, while the Ni and Co are the SC elements and the corresponding content values are determined by C_{Cr} as $C_{Ni} = C_{Co} = (75\ \text{at\%} - C_{Cr})/2$. Consequently, the content variations in Ni, Cr, and Co elements for different MC element are list in Table 1. Obviously, the analyzed samples are small and characterized by multiple independent variables that exhibit correlation within each sample. Therefore, the numerical analysis problem addressed in this paper is well suited for employing the PLS method to establish regression models, enabling an insightful examination of the influence of various alloying elements on the intrinsic properties of $Al_{10}Ti_{15}Ni_{x1}Cr_{x2}Co_{x3}$ alloys and unveiling the competitive mechanisms among these elements.

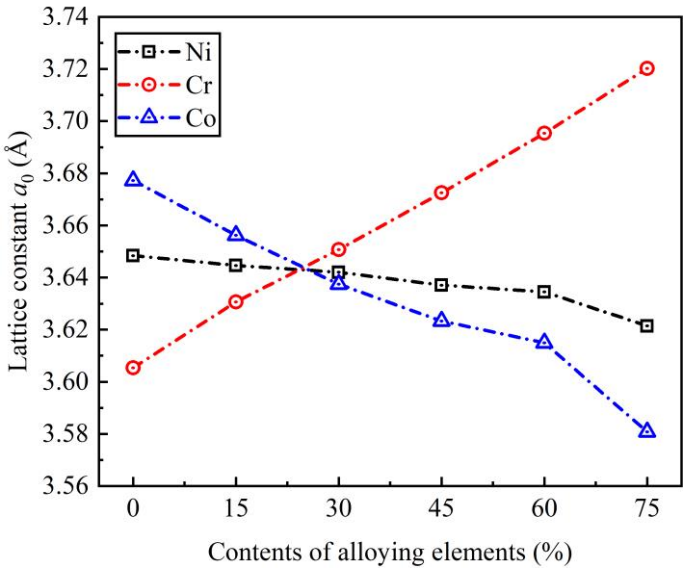

Figure 1. The relationships between the lattice constant a_0 and the content of different MC elements in $Al_{10}Ti_{15}Ni_{x1}Cr_{x2}Co_{x3}$ alloys.

Table 1. The variations in Ni, Cr, and Co contents under different MC elements.

MC Element Ni			MC Element Cr			MC Element Co		
C_{Ni} (at%)	C_{Cr} (at%)	C_{Co} (at%)	C_{Ni} (at%)	C_{Cr} (at%)	C_{Co} (at%)	C_{Ni} (at%)	C_{Cr} (at%)	C_{Co} (at%)
0	37.5	37.5	37.5	0	37.5	37.5	37.5	0
15	30	30	30	15	30	30	30	15
30	22.5	22.5	22.5	30	22.5	22.5	22.5	30
45	15	15	15	45	15	15	15	45
60	7.5	7.5	7.5	60	7.5	7.5	7.5	60
75	0	0	0	75	0	0	0	75

3. Results and Discussions

To compare the disparities between SE and ME analyses for the same alloying element, the lattice constant a_0 of $Al_{10}Ti_{15}Ni_{x1}Cr_{x2}Co_{x3}$ alloys is initially determined by the EMTO-CPA method. Subsequently, the relationships between the lattice constant a_0 and the content of Ni, Cr, and Co elements are individually obtained, as shown in Figure 1. The three curves in the figure correspond to only one MC element, namely Ni, Cr, and Co, while the homologous SC elements are not displayed. Clearly, the a_0 value shows an almost linear increase with the rise in Cr content, and gradually decreases with the augmentation of Ni or Co content. The results demonstrate a positive correlation between the lattice constant a_0 and the Cr content, while exhibiting a negative correlation with the Ni and Co contents. The observed trend can be attributed to the relatively larger atomic radius of the Cr element in comparison to the relatively smaller atomic radii of Ni and Co elements. At the same time, it can be seen that the value of a_0 presents a more pronounced decline with increasing Co content compared to the increase observed with Ni content, indicating that the presence of the Co element has a stronger negative influence on the lattice constant of alloys. In general, the Cr element exhibits a pronounced positive influence on the lattice constant of alloys, whereas Ni and Co elements exert an opposing effect, with Co demonstrating a more substantial negative impact.

Obviously, the analysis of each curve is exclusively focused on the impact of varying the content of one MC element, disregarding any corresponding changes in SC elements and thus failing to account for their combined effect on the lattice constant of $Al_{10}Ti_{15}Ni_{x1}Cr_{x2}Co_{x3}$ alloys. Meanwhile, it is evident from Table 1 that the contents of SC elements exhibit significant variations in accordance with the content of MC element. Therefore, it is imperative to concurrently consider the combined influence of variation in the content of the three alloying elements Ni, Cr, and Co on the lattice constant in $Al_{10}Ti_{15}Ni_{x1}Cr_{x2}Co_{x3}$ alloys. Herein, the PLS regression is employed to explore deeper layers of information to fulfill this objective [41]. The optimal number of principal components is initially determined as 1 through cross-validation analysis based on the data results presented in Figure 1 and Table 1. Subsequently, regression analysis is conducted, and the corresponding findings are summarized in Table 2.

Table 2. The PLS regression results between the content of Ni, Cr, and Co elements and the lattice constant a_0.

Independent Variables	Dependent Variable	Standardized Regression Coefficients	Projected Importance Indexes	R^2 Value (%)
C_{Ni}	a_0	−0.150	0.320	98.6
C_{Cr}		0.633	1.353	
C_{Co}		−0.484	1.033	

In the regression analysis, the content of Ni, Cr, and Co elements is set as the independent variable, and the value of lattice constant a_0 is regarded as the dependent variable. The standardized regression coefficient serves as a metric for assessing the relative influence of

the independent variable on the dependent variable, and the larger the absolute value of the coefficient, the more significant its impact becomes. The projected importance index quantifies the explanatory ability of the independent variable to the dependent variable, with a higher value indicating a stronger ability to explain. The R^2 value, in addition, serves as an indicator of the goodness of fit for the PLS regression model, with a higher value indicating a stronger fit degree. In light of the analysis results, the standardized regression coefficients of Ni, Cr and Co elements are −0.15, 0.633 and −0.484, respectively. Hence, the standardized regression relationship between the a_0 and the C_{Ni}, C_{Cr}, C_{Co} can be formulated as $a_0 = -0.15C_{Ni} + 0.633C_{Cr} - 0.484C_{Co}$. The result indicates that the Cr element exerts the most significant positive influence on the formation of lattice constant a_0 in the $Al_{10}Ti_{15}Ni_{x1}Cr_{x2}Co_{x3}$ alloys, whereas the Ni an Co elements exhibit an opposing effect, and the Co element displays a larger magnitude of negative impact. Meanwhile, Figure 2 provides a visual representation illustrating the varying degrees of impact for better understanding. Herein, the absolute value of regression coefficient quantifies the degree of influence exerted by each alloying element on the lattice constant, aligning consistently with the atomic radius of these three alloying elements, and the positive and negative signs well reflect the influence direction of each element. Meanwhile, the corresponding values of projected importance indexes, respectively, are 0.32, 1.353 and 1.033, showing that the Cr and Co elements significantly contributes to the construction of the regression expression, whereas the influence of the Ni element is comparatively minor. However, on the whole, the regression expression exhibits a robust fit with the experimental data for the independent variables C_{Ni}, C_{Cr}, C_{Co} and the dependent variable a_0, as indicated by an impressive R^2 value of 98.6%. Consequently, it follows that the influence trend of the same alloying element on the lattice constant shows no significant difference between SE and ME analyses.

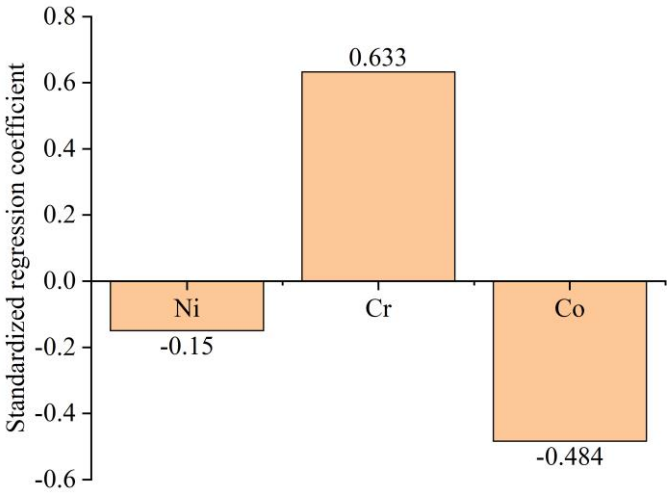

Figure 2. Histogram of standardized regression coefficients for Ni, Cr and Co elements with respect to a_0.

To further investigate potential disparities, additional significant physical properties, namely the elastic constants C_{11}, C_{12} and C_{44}, are calculated, and the relationships between the elastic constants and the content of MC elements, Ni, Cr, Co, are depicted in Figure 3. Evidently, the influence of increasing the content of a certain MC element on the C_{11} and C_{44} exhibits similarity. The values of C_{11} and C_{44} exhibited an overall upward trend with the increase in Ni, Cr, or Co content. The influence of Co is the most pronounced among them, while the influences of Cr and Ni decrease sequentially, with a particular flattening out observed in higher Ni content, as shown in Figure 3a,c. However, the fluctuation of elastic constant C_{12} exhibits a higher degree of complexity, as illustrated in Figure 3b. When the content of MC element is low, there is a rapid decline in the value of C_{12} with an increase in Ni or Cr content, while the influence of Co content remains relatively constant.

Meanwhile, the influence of the Co element is most pronounced when the content of MC element is high, whereas the impacts of Cr and Ni elements are relatively insignificant. To summarize, in the analysis of a single element, the influences of Ni, Cr, and Co on C_{11} and C_{44} are successively amplified, while their effects on C_{12} do not exhibit a prominent regularity.

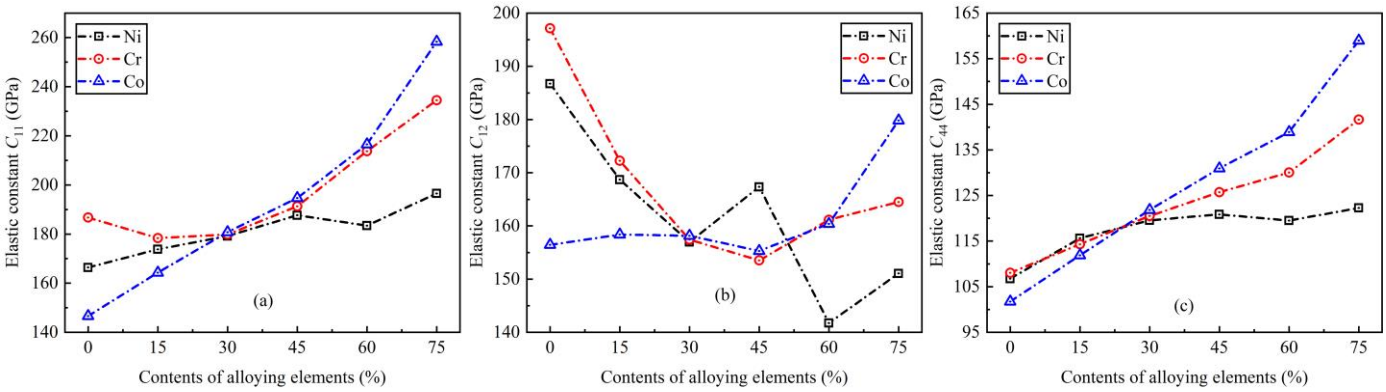

Figure 3. The relationships between the elastic constants and the content of different MC elements in $Al_{10}Ti_{15}Ni_{x1}Cr_{x2}Co_{x3}$ alloys: (**a**) C_{11}, (**b**) C_{12}, and (**c**) C_{44}.

At the same time, the competitive relationships between Ni, Cr, and Co elements are further elucidated through the implementation of ME analysis based on the PLS regression, as listed in Table 3. According to the calculated results, the standardized regression relationships between the dependent variables C_{11}, C_{12}, C_{44} and the independent variables C_{Ni}, C_{Cr}, C_{Co} could be formulated as follows

$$\begin{cases} C_{11} = -0.463C_{Ni} - 0.101C_{Cr} + 0.480C_{Co} \\ C_{12} = -0.447C_{Ni} - 0.184C_{Cr} + 0.528C_{Co} \\ C_{44} = -0.495C_{Ni} - 0.153C_{Cr} + 0.511C_{Co} \end{cases} \quad (1)$$

in which, the standardized regression coefficients corresponding to the content of Ni, Cr, and Co elements are utilized as the coefficient values preceding the independent variables, and the coefficients reflect the influence trend of the independent variables on the dependent variable.

Table 3. The PLS regression results between the content of Ni, Cr, and Co elements and the elastic constants.

Independent Variables	Dependent Variables			Standardized Regression Coefficients			Projected Importance Indexes			R^2 Values (%)		
C_{Ni}				−0.463	−0.447	−0.495	1.213	1.021	1.228			
C_{Cr}	C_{11}	C_{12}	C_{44}	−0.101	−0.184	−0.153	0.284	0.336	0.214	72.5	75.3	76.1
C_{Co}				0.480	0.528	0.511	1.227	1.358	1.252			

To intuitively observe the different influence trends, a corresponding histogram is illustrated in Figure 4. Overall, based on the regression analysis results, it can be inferred that the presence of the Co element exerts a significant positive influence on the elastic constants C_{11}, C_{12} and C_{44}, and the result is consistent with the SE analysis in Figure 3. Meanwhile, the Ni and Cr elements demonstrate a negative effect on the elastic constants in general; the adverse impact of the Ni element is particularly significant, and that of the Cr element is small. Therefore, a noteworthy phenomenon can be observed when comparing the outcomes depicted in Figures 3 and 4. It can be seen that the augmentation of Ni and Cr content is observed to positively impact the values of C_{11} and C_{44} in the SE analysis, while the ME analysis reveals a negative promoting effect of the two alloying

elements. The analysis of the curves in Figure 3 reveals that the positive promoting effect of Ni and Cr elements is not superior to that of the Co element, and the influence of Cr and Ni elements exhibit a gradual decrease in succession. Consequently, a subsequent regression analysis reveals the latent competitive relationship among the various alloying elements concerning the elastic constants as shown in Figure 4. In Table 3, the projected importance indexes represent the explanatory power of independent variables on their corresponding dependent variables, as previously mentioned. And the corresponding R^2 values, respectively, are 72.5%, 75.3% and 76.1%, indicating that the fitting degree of regression equations are relatively good, the intricate numerical relationship between the content of alloying elements and the elastic constants in Figure 3 lead to the results, and ignoring the role of Al and Ti elements may also have some influence. This issue needs further investigation. However, the outcomes of the competition among multiple alloying elements remain valuable as a point of reference.

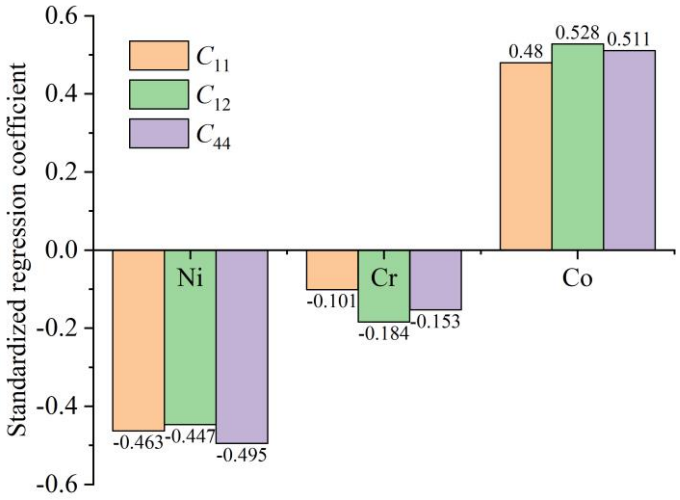

Figure 4. Histogram of standardized regression coefficients for Ni, Cr and Co elements with respect to the elastic constants.

Elastic moduli, including bulk modulus B, shear modulus G, and Young's modulus E, are further determined to facilitate a comparative analysis of the impact of alloying elements in the SE and ME analyses. The relationships between the content of MC elements and the elastic moduli are illustrated in Figure 5. For the bulk modulus B, the corresponding curves display a complex trend of variation as the content of one MC element increases, as shown in Figure 5a. The B value exhibits an initial decrease followed by an increase as the Ni or Cr content increases, while the overall trend rises with the increase in Co content. Therefore, it can be predicted that the promoting effect of the three alloying elements on the bulk modulus B is positive for the Co element, negative for the Ni element, and inconclusive for the Cr element. Meanwhile, the variation in curves exhibits similar regularities in Figure 5b,c, and the values of G and E gradually rise with the increase in one MC content. And the influence trend of the three alloying elements is similar at low content, while the impact of the Co element becomes predominant at high concentrations. Therefore, the SE analysis demonstrates that augmenting the Co content among the three alloying elements is more conducive to improving the elastic moduli of $Al_{10}Ti_{15}Ni_{x1}Cr_{x2}Co_{x3}$ alloys.

In order to further elucidate the competitive relationship among the three alloying elements on the elastic moduli of alloys, a ME analysis based on the PLS regression is conducted using the data presented in Table 1 and Figure 5, and the corresponding results are summarized in Table 4. As mentioned above, the standardized regression relationships between the dependent variables B, G, E and the independent variables C_{Ni}, C_{Cr}, C_{Co} could be formulated as follows

$$\begin{cases} B = -0.427C_{Ni} + 0.191C_{Cr} + 0.498C_{Co} \\ G = -0.405C_{Ni} + 0.104C_{Cr} + 0.421C_{Co} \\ E = -0.398C_{Ni} + 0.108C_{Cr} + 0.425C_{Co} \end{cases} \quad (2)$$

where the coefficients associated with C_{Ni}, C_{Cr}, and C_{Co} in the equations correspond to the standardized regression coefficients presented in the table. The absolute value of coefficients reflects the intensity of competition among the three alloying elements, while the positive and negative signs signify the direction of their respective influences.

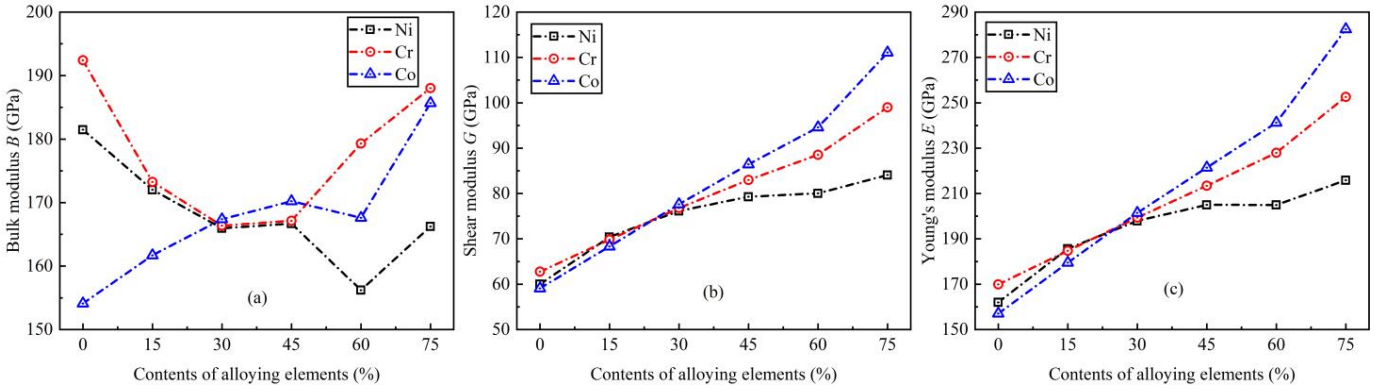

Figure 5. The relationships between the elastic moduli and the content of different MC elements in $Al_{10}Ti_{15}Ni_{x1}Cr_{x2}Co_{x3}$ alloys: (**a**) *B*, (**b**) *G*, and (**c**) *E*.

Table 4. The PLS regression results between the content of Ni, Cr, and Co elements and the elastic moduli.

Independent Variables	Dependent Variables			Standardized Regression Coefficients			Projected Importance Indexes			R^2 Values (%)		
C_{Ni}				−0.427	−0.405	−0.398	1.134	1.127	1.115			
C_{Cr}	*B*	*G*	*E*	0.191	0.104	0.108	0.357	0.325	0.320	79.4	70.6	71.5
C_{Co}				0.498	0.421	0.425	1.326	1.302	1.315			

At the same time, the bar chart in Figure 6 clearly presents the regression coefficients, facilitating a better understanding of the competitive relationship among alloying elements. Evidently, the positive coefficients for Cr and Co indicate that increasing their content is advantageous in enhancing the elastic moduli of alloys, particularly with a more pronounced effect observed for higher Co content due to its larger corresponding coefficient value. The result is consistent with the influence trend of the Co element predicted by SE analysis, and clearly illustrate the uncertain impact of the Cr element in Figure 5. For the Ni element, it can be seen that the coefficient values are all negative, showing that the addition of Ni content is not conducive to improving the elastic moduli of alloys. In which, the coefficient of −0.427 aligns well with the predicted trend of the Ni element on the bulk modulus *B* in Figure 5a. And the coefficients of −0.405 and −0.398 indicate a hidden competitive relationship in Figure 5a,c, showing that while the influences of the Ni element on the *G* and *E* are upward in the SE analysis, it should be downward when considering the combined effect of three alloying elements in the ME analysis, the observed outcome is attributed to the altering of Ni content in $Al_{10}Ti_{15}Ni_{x1}Cr_{x2}Co_{x3}$ alloys while disregarding its impact on the Cr and Co contents. And the height of the histogram directly reflects the competitive relationship among the three alloy elements. It is evident that Co and Ni exhibit strong competitive advantages, albeit in opposite directions, while Cr demonstrates relatively weaker competitiveness, suggesting that increasing Co content or reducing Ni content can significantly enhance the elastic moduli of $Al_{10}Ti_{15}Ni_{x1}Cr_{x2}Co_{x3}$ alloys. Moreover, the R^2 values reflect the fitting degree of the corresponding regression expressions as 79.4%, 70.6%, and 71.5%, respectively. The degree of fit is not optimal, as it is determined by the intricate

interplay of data relationships. However, the results still hold some theoretical reference value in terms of revealing the competitive relationship between various alloying elements and promoting the mechanical properties of alloy materials.

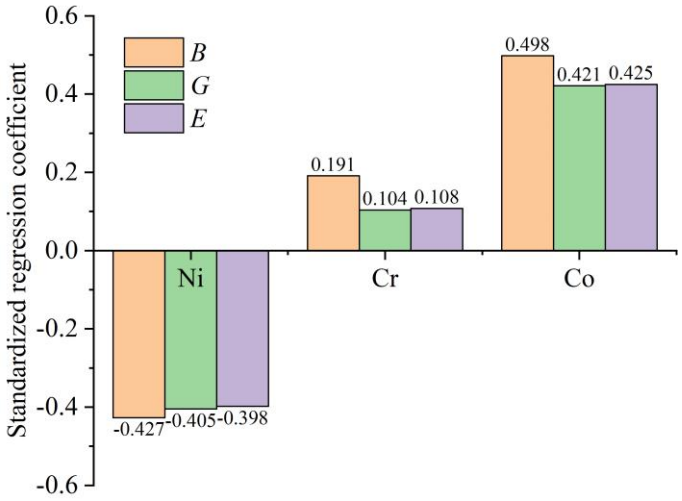

Figure 6. Histogram of standardized regression coefficients for Ni, Cr and Co elements with respect to the elastic moduli.

4. Conclusions

In summary, the competitive mechanisms between Ni, Cr, and Co elements on the physical properties of $Al_{10}Ti_{15}Ni_{x1}Cr_{x2}Co_{x3}$ alloys are investigated through SE and ME analyses based on first principles calculations and PLS regression. The key findings are outlined as follows:

The increase in Ni or Co content in the $Al_{10}Ti_{15}Ni_{x1}Cr_{x2}Co_{x3}$ alloys leads to a_0 reduction, whereas the opposite effect is observed with the addition of the Cr element in light of SE analysis. Meanwhile, the ME analysis reveals that the Cr element exhibits the most significant competitive advantage among the three alloying elements, with a positive promotion direction, while the Ni and Co elements demonstrate a negative effect, which aligns with SE analysis.

The SE analysis suggests that augmenting the contents of Ni, Cr, and Co elements can effectively enhance the values of C_{11} and C_{44}, while the impact on the elastic constant C_{12} remains inconclusive. Further analysis using ME revealed the competitive relationship among the three alloying elements in the formation of elastic constants, with negative effects observed for Ni and Cr elements, while a positive effect is observed for the Co element. Moreover, both Ni and Co elements exhibited strong competitive strength, but their competitive directions are opposite.

The SE analysis reveals a positive promotional effect of the Ni, Cr, Co elements on the elastic moduli *G* and *E*. However, a negative influence of the Ni element on the elastic moduli *B*, *G* and *E* is observed through the ME analysis. Additionally, it is observed that there is a gradual decline in the level of competitiveness among the elements Co, Ni, and Cr.

Among them, the SE analysis and ME analysis yield some different conclusions, the reason is that the SE analysis solely takes into account the impact of variations in the content of a single alloying element, while disregarding the influence on the content of other alloying elements and subsequently neglecting their collective effect on the physical properties of alloys. Therefore, merely employing the first principles calculations is inadequate for comprehensively investigating the influence of alloying element content on the physical properties of alloy materials, but using multivariate numerical analysis will be more helpful to reveal the hidden interaction mechanism. The present study provides a novel research concept to elucidate the competitive relationship among alloying elements, thereby offering more reliable theoretical guidance for the development of new alloy materials.

Author Contributions: Writing—original draft preparation, software, methodology, formal analysis, and data curation, Y.L.; investigation, L.W. and J.Z.; writing—review and editing, software, and methodology, Z.W.; writing—review and editing and resources, R.Z. and Y.W.; software, T.F. and P.T. All authors have read and agreed to the published version of the manuscript.

Funding: The authors are grateful for the financial support from the National Natural Science Foundation of China (52171115), the Natural Science Foundation of Hunan Province (2021JJ40035, 2021JJ50086, 2023JJ50114), the Scientific Research Fund of Hunan Provincial Education Department (22B0860, 22A0627), the Changsha Municipal Natural Science Foundation (kp2202155), the Technological Innovation Projects of Hengyang (202250045149), and the Scientific Research Project of Hunan Institute of Technology (KFKA2202, KFA23015, HQ22014, HG-SYL3-021, and S202311528137).

Institutional Review Board Statement: Not applicable.

Informed Consent Statement: Not applicable.

Data Availability Statement: The data presented in this study are not available due to privacy.

Acknowledgments: The authors deeply appreciate Levente Vitos for providing his developed codes of EMTO-CPA method for this work.

Conflicts of Interest: The authors declare no conflicts of interest.

References

1. Zhang, Z.; Li, Y.; Liu, Y.; Li, H.; Zhang, D.; Zhang, J. A novel Al-Mg-Zn(-Cu) crossover alloy with ultra-high strength. *Mater. Lett.* **2023**, *347*, 134640. [CrossRef]
2. Ma, Y.; Liu, C.; Jiang, S.; Wan, Y.; Gao, Y.; Chen, Z.; Liu, Z. Achieving high strength-ductility synergy in a dilute Mg-Gd-Zn-Zr alloy with heterogeneous structure via hot extrusion. *J. Mater. Res. Technol.* **2023**, *27*, 1509–1525. [CrossRef]
3. Mao, J.; Wen, S.; Liang, S.; Wu, X.; Wei, W.; Huang, H.; Gao, K.; Nie, Z. Precipitation behaviors and thermal stability of Al-3.5Mg-1.0Cu alloy with co-addition of Zn and Si. *J. Alloys Compd.* **2023**, *946*, 169401. [CrossRef]
4. Li, J.; Liu, Z.; Ning, H.; Ma, H.; Xie, R.; Kong, Y.; Fu, Y. Ni-based coating on 5083 aluminum alloy with Cu-Ni interlayer fabricated by ultra-high-speed laser directed energy deposition. *Surf. Coat. Technol.* **2023**, *474*, 130068. [CrossRef]
5. Liu, Z.C.; Kong, D.J. Effects of TiC mass fraction on microstructure, corrosive-wear and electrochemical properties of laser cladded CoCrFeNiMo high-entropy alloy coatings. *Tribol. Int.* **2023**, *186*, 108640.
6. Shao, Q.; Elgallad, E.M.; Maltais, A.; Chen, X.G. Development of thermal-resistant Al-Zr based conductor alloys via microalloying with Sc and manipulating thermomechanical processing. *J. Mater. Res. Technol.* **2023**, *25*, 7528–7545. [CrossRef]
7. Huang, Y.F.; Lei, J.D.; Chen, H.Y.; Zhou, Z.Y.; Dong, H.L.; Yang, S.Q.; Gao, H.T.; Wei, T.R.; Zhao, K.P.; Shi, X. Intrinsically high thermoelectric performance in near-room-temperature a-MgAgSb materials. *Acta Mater.* **2023**, *249*, 118847. [CrossRef]
8. Sui, Q.; Wang, Z.; Wang, J.; Xu, S.; Yuan, Q.; Wen, H.; Xiao, T.; Liu, J. Phase evolution and mechanical properties of AlxCoCrFeNi high-entropy alloys by directed energy deposition. *Mater. Charact.* **2023**, *204*, 113217. [CrossRef]
9. Chu, C.H.; Guo, Q.Y.; Ding, R.; Liu, Y.C. The effects of Ti and Ta on the microstructure and high temperature deformation mechanisms of the CoNi-based superalloys. *Mater. Charact.* **2023**, *199*, 112841. [CrossRef]
10. Li, X.; Zhao, Q.; Tian, Y.; Wang, Q.; Fan, J.; Song, K.; Zhou, H.; Wang, J. Phase transformation induced transitional twin boundary in body-centered cubic metals. *Acta Mater.* **2023**, *249*, 118815. [CrossRef]
11. Jian, Y.; Qi, H.; Zhang, J.; Kong, H.; Huang, Z.; Xing, J. Effects of trace Si addition on the microstructure evolution and mechanical properties of MoAlB ceramic. *J. Alloys Compd.* **2023**, *941*, 168873. [CrossRef]
12. Liu, X.W.; Xie, L.J.; Wang, Y.S.; Yao, J.Q.; Zhu, C.; Fan, S.; Ma, X.N.; Cao, H.T. Grain refinement of an as-cast CoCrNi multi-principal element alloy by inducing solute segregation: Solute design and effects. *Metall. Mater. Trans. A* **2023**, *54*, 3742–3751. [CrossRef]
13. Hu, C.; Zhang, J.; Zhang, Y.; Song, C.; Zhai, Q. A great enhancement of both strength and plasticity in a dual-phase high-entropy alloy by multi-effects of high carbon addition. *Mater. Des.* **2023**, *225*, 111571. [CrossRef]
14. Lv, Y.K.; Zhao, X.R.; Shi, T.; Bai, L.; Chen, J.; Wang, X.H. Excellent room temperature ductility of as-cast TRIP high-entropy alloy via Mo and C alloying. *J. Mater. Sci.* **2020**, *55*, 2239–2244. [CrossRef]
15. Tong, Y.; Chen, D.; Han, B.; Wang, J.; Feng, R.; Yang, T.; Zhao, C.; Zhao, Y.; Guo, W.; Shimizu, Y.; et al. Outstanding tensile properties of a precipitation-strengthened $FeCoNiCrTi_{0.2}$ high-entropy alloy at room and cryogenic temperatures. *Acta Mater.* **2019**, *165*, 228–240. [CrossRef]
16. Wu, X.; Guan, Z.-P.; Yang, Z.-Z.; Wang, X.; Qiu, F.; Wang, H.-Y. Effect of Cu content on central-segregation composition and mechanical properties of Al–Mg–Si alloys produced by twin-roll casting. *Mater. Sci. Eng. A* **2023**, *869*, 144782. [CrossRef]
17. Li, L.L.; Li, Z.M.; Da Silva, A.K.; Peng, Z.R.; Zhao, H.; Gault, B.; Raabe, D. Segregation-driven grain boundary spinodal decomposition as a pathway for phase nucleation in a high-entropy alloy. *Acta Mater.* **2019**, *178*, 1–9. [CrossRef]
18. Hou, P.Y. Segregation phenomena at thermally grown Al_2O_3/alloy interfaces. *Annu. Rev. Mater. Res.* **2008**, *38*, 275–298. [CrossRef]
19. Su, J.; Guo, F.; Gao, X.B.; Feng, H.Q. Study on solid-solution interaction and existing forms of alloying elements in Mg–Al–Zn-Gd alloy. *J. Alloys Compd.* **2021**, *854*, 156209.

20. Lin, M.; Yang, Z.; Shi, X.; Chen, Y.; Lu, J.; Wang, Z.; Li, J.; Wang, J.; He, F. Effective combination of solid solution strengthening and precipitation hardening in NiCrFeWTiAl multi-principal element alloys. *J. Alloys Compd.* **2023**, *933*, 167738. [CrossRef]
21. Zhang, H.; Yang, D.; Chen, X.; Nagaumi, H.; Wu, Z.; Guo, C.; Zou, J.; Wang, P.; Qin, K.; Cui, J. Influence of Ag on microstructure, mechanical properties and tribological properties of as-cast Al-33Zn-2Cu high-zinc aluminum alloy. *J. Alloys Compd.* **2022**, *922*, 166157. [CrossRef]
22. Ye, X.-C.; Wang, T.; Xu, Z.-Y.; Liu, C.; Wu, H.-H.; Zhao, G.-W.; Fang, D. Effect of Ti content on microstructure and mechanical properties of CuCoFeNi high-entropy alloys. *Int. J. Miner. Metall. Mater.* **2020**, *27*, 1326–1331. [CrossRef]
23. Nguyen, T.; Huang, M.; Li, H.; Hong, L.; Yang, S. Effect of Al content on microstructure and mechanical properties of as-cast $Al_xFeMnNiCrCu_{0.5}$ high-entropy alloys. *Mater. Sci. Eng. A* **2022**, *832*, 142495. [CrossRef]
24. Luo, X.; Feng, J.; Liu, Y.-H.; Hu, M.-Y.; Chong, X.-Y.; Jiang, Y.-H. Properties of Fe–Mn–Al alloys with different Mn contents using density functional theory. *Rare Met.* **2023**, *42*, 1387–1397. [CrossRef]
25. Liu, Y.; Liu, W.; Zhou, Q.Y.; Liu, C.; Fan, T.W.; Wu, Y.Z.; Wang, Z.P.; Tang, P.Y. An initio study of thermodynamic and fracture properties of CrFeCoNiMn ($0 \leq x \leq 3$) high-entropy alloys. *J. Mater. Res. Technol.* **2022**, *17*, 498–506. [CrossRef]
26. Wang, H.; Wang, C.Y.; Liang, J.X.; Godfrey, A.; Wang, Y.H.; Weng, Y.Q.; Cao, W.Q. Effect of alloying content on microstructure and mechanical properties of Fe-Mn-Al-C low-density steels. *Mater. Sci. Eng. A* **2023**, *886*, 145675. [CrossRef]
27. Wang, S.; Li, J.; Li, D. First-principle study on physical properties and vacancy formation of face-centered cubic Co-Ni-Cu-Mo-W high entropy alloys. *J. Mater. Res. Technol.* **2023**, *25*, 5483–5493. [CrossRef]
28. Fan, Q.C.; Li, B.S.; Zhang, Y. Influence of Al and Cu elements on the microstructure and properties of $(FeCrNiCo)Al_xCu_y$ high-entropy alloys. *J. Alloys Compd.* **2014**, *614*, 203–210. [CrossRef]
29. Vitos, L. *Computational Quantum Mechanics for Materials Engineers: The EMTO Method and Applications*; Springer: London, UK, 2007.
30. Soven, P. Coherent-potential model of substitutional disordered alloys. *Phys. Rev. B* **1967**, *156*, 809–813. [CrossRef]
31. Gyorffy, B.L. Coherent-potential approximation for a nonoverlapping-muffin-tin-potential model of random substitutional alloys. *Phys. Rev. B* **1972**, *5*, 2382–2384. [CrossRef]
32. Tian, F.; Varga, L.K.; Chen, N.; Delczeg, L.; Vitos, L. Ab initio investigation of high-entropy alloys of 3d elements. *Phys. Rev. B* **2013**, *87*, 075144. [CrossRef]
33. Kohn, W.; Sham, L.J. Self-consistent equations including exchange and correlation effects. *Phys. Rev.* **1965**, *140*, A1133–A1138. [CrossRef]
34. Vitos, L.; Kollár, J.; Skriver, H.L. Full charge-density calculation of the surface energy of metals. *Phys. Rev. B* **1994**, *49*, 16694–16701. [CrossRef] [PubMed]
35. Perdew, J.P.; Burke, K.; Ernzerhof, M. Generalized gradient approximation made simple. *Phys. Rev. Lett.* **1996**, *77*, 3865–3868. [CrossRef] [PubMed]
36. Gyorffy, B.L.; Pindor, A.J.; Staunton, J.; Stocks, G.M.; Winter, H. A first-principles theory of ferromagnetic phase transitions in metals. *J. Phys. F Met. Phys.* **1985**, *15*, 1337–1386. [CrossRef]
37. Zoubi, N.I.A.; Punkkinen, M.P.J.; Johansson, B.; Vitos, L. Completeness of the exact muffin-tin orbitals: Application to hydrogenated alloys. *Phys. Rev. B* **2010**, *81*, 045122. [CrossRef]
38. Korzhavyi, P.A.; Ruban, A.V.; Abrikosov, I.A.; Skriver, H.L. Madelung energy for random metallic alloys in the coherent potential approximation. *Phys. Rev. B* **1995**, *51*, 5773–5780. [CrossRef] [PubMed]
39. Tian, F.; Delczeg, L.; Chen, N.; Varga, L.K.; Shen, J.; Vitos, L. Structural stability of $NiCoFeCrAl_x$ high-entropy alloy from ab initio theory. *Phys. Rev. B* **2013**, *88*, 085128. [CrossRef]
40. Girifalco, L.; Weizer, V. Application of the morse potential function to cubic metals. *Phys. Rev. B* **1959**, *114*, 687–690. [CrossRef]
41. Wold, S.; Sjöström, M.; Eriksson, L. PLS-regression: A basic tool of chemometrics. *Chemom. Intell. Lab. Syst.* **2001**, *58*, 109–130. [CrossRef]
42. Faul, F.; Erdfelder, E.; Buchner, A.; Lang, A.-G. Statistical power analyses using G*Power 3.1: Tests for correlation and regression analyses. *Behav. Res. Methods* **2009**, *41*, 1149–1160. [CrossRef] [PubMed]
43. Wan, X.; Wang, Y.; Zhao, D. Multi-response optimization in small scale resistance spot welding of titanium alloy by principal component analysis and genetic algorithm. *Int. J. Adv. Manuf. Technol.* **2016**, *83*, 545–559. [CrossRef]
44. Hardoon, D.R.; Szedmak, S.; Shawe-Taylor, J. Canonical correlation analysis: An overview with application to learning methods. *Neural Comput.* **2004**, *16*, 2639–2664. [CrossRef] [PubMed]
45. Chong, I.-G.; Jun, C.-H. Performance of some variable selection methods when multicollinearity is present. *Chemom. Intell. Lab. Syst.* **2005**, *78*, 103–112. [CrossRef]